Science of the Total Environment 888 (2023) 164193

Contents lists available at ScienceDirect

Science of the Total Environment

journal homepage: www.elsevier.com/locate/scitotenv

40 years of changes in sea surface temperature along the Western Iberian Coast

Beatriz Biguino [a,*], Carlos Antunes [b,c], Luísa Lamas [d], Luke J. Jenkins [e], João Miguel Dias [f], Ivan D. Haigh [e], Ana C. Brito [a,g]

[a] Marine and Environmental Sciences Centre (MARE), Aquatic Research Network (ARNET), Faculdade de Ciências, Universidade de Lisboa, 1749-016 Lisboa, Portugal
[b] Instituto Dom Luiz (IDL), Universidade de Lisboa, 1749-016 Lisboa, Portugal
[c] Departamento de Engenharia Geográfica, Geofísica e Energia, Faculdade de Ciências, Universidade de Lisboa, 1749-016 Lisboa, Portugal
[d] Instituto Hidrográfico (IH), Rua das Trinas 49, 1249-093 Lisboa, Portugal
[e] School of Ocean and Earth Science, University of Southampton, National Oceanography Centre, Waterfront Campus, European Way, Southampton SO14 3ZH, UK
[f] Centre for Environmental and Marine Studies (CESAM), Departamento de Física, Universidade de Aveiro, 3810-193 Aveiro, Portugal
[g] Departamento de Biologia Vegetal, Faculdade de Ciências, Universidade de Lisboa, 1749-016 Lisboa, Portugal

HIGHLIGHTS

- Global *SST* is increasing but coastal regional trends are not fully understood
- *SST* changes along the Western Iberian Coast were assessed using 40 years of data.
- *SST* has been increasing along the Western Iberian Coast (0.10–0.25 °C/decade).
- The *SST* increase has been decelerating in recent decades along this region.
- No changes were observed near shore, likely due to upwelling and *NAO*/*WeMOI* effects.

GRAPHICAL ABSTRACT

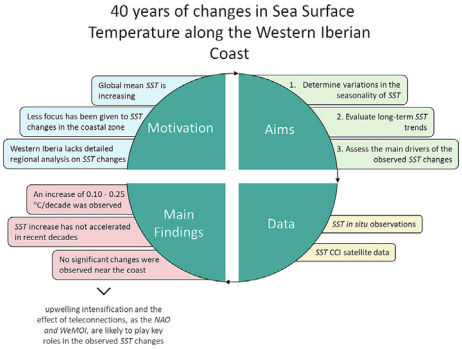

ARTICLE INFO

Editor: Martin Drews

Keywords:
Rising temperatures
Climate change
Ocean-atmosphere interactions
Buffer effect
Trends
Anomalies
Seasonality variability

ABSTRACT

Climate change is causing mean sea surface temperatures (*SST*) to increase worldwide. However, this increase has not been temporally or spatially uniform, with variations observed depending both on the period considered and the geographic region. In this context, this paper aims to quantify relevant changes in *SST* along the Western Iberian Coast over the last four decades, through the calculation of trends and anomalies of long-term time series of *in situ* observations and satellite-derived data. Potential drivers of *SST* changes were considered using atmospheric and teleconnections time series. Changes in the seasonal cycle of *SST* were also evaluated.

We show that *SST* has increased since 1982, with regional variations between 0.10 and 0.25 °C per decade, with an increase in air temperature appearing to drive the *SST* trends along the Iberian coast. In the near-shore area, no significant trends or changes in the seasonal cycle of *SST* were observed, which is likely due to a buffer effect caused by the seasonal upwelling that characterizes the region. Recent decades show a slowdown in the increase rate of *SST* along the Western Iberian Coast. An upwelling intensification could justify this observation, along with the effect of teleconnections on the regional climate, such as the North Atlantic Oscillation (*NAO*) and the Western Mediterranean Oscillation Index (*WeMOI*). Our results suggest that the *WeMOI* plays a more important role in coastal *SST* variability than the other teleconnections.

* Corresponding author.
E-mail address: bibiguino@fc.ul.pt (B. Biguino).

http://dx.doi.org/10.1016/j.scitotenv.2023.164193
Received 2 March 2023; Received in revised form 21 April 2023; Accepted 11 May 2023
Available online 15 May 2023

The present study quantifies regional changes in *SST* and enhances knowledge of the role of ocean-atmosphere interactions in regulating climate and weather conditions. Moreover, it provides a relevant scientific context to the development of regional adaptative and mitigation actions in response to climate change.

1. Introduction

Global mean sea surface temperature (*SST*) has been increasing in past decades, as anthropogenic pressures induce climate change (IPCC, 2021). Between 1993 and 2017, the rate of ocean warming, and thus heat uptake, rose to 6.28 ± 0.48 ZJ/year (for the first 700 m), approximately equivalent to a warming of 0.044 °C for the first 100 m of water depth (IPCC, 2019). Wu et al. (2020) found an increase of 0.035 °C/decade between 1854 and 2017 for the surface of the global ocean, that has been accelerating in the most recent years (0.102 °C/decade between 1988 and 2017 and 0.274 °C/decade between 2008 and 2017). This temperature increase, at the surface and at depth, is driving ocean acidification, sea level rise, marine heat waves and the growth of the number of weather hazards on the ocean, which directly affects coastal populations and ecosystems (Wu et al., 2020). *SST* variations influence ocean circulation, nutrient fluxes and primary production, which consequently affect carbon fluxes. It can impact species abundance, distribution and behavior, affecting coastal populations that depend on fisheries or maritime tourism (Minnett et al. (2019); Hastings et al. (2020); EPA (2022a)). *SST* also regulates climate and provides information about ocean-atmosphere interactions. Therefore, as all processes in nature show a relation with temperature (Minnett et al., 2019), monitoring *SST* variations is critical, especially in the context of climate change, with models predicting that *SST* will continue to increase into the future (Ruela et al., 2020).

Although it is well-established that mean *SST* is increasing in the global ocean, far less focus has been given to changes in the coastal zone. In the coastal zone, a wider range of variation in trends has been observed and regional variations are still not fully understood. Furthermore, changes in the seasonality of *SST* have been shown to be important, as they can induce variations in seasonal activities and in the timing of seasonal life cycles (phenology) of several species (IPCC, 2019, 2021). It is the finer detail of regional analysis that allows an improved understanding of climate change, choice of adaptation strategies and mitigation plans tailored to the different ecosystem and populational contexts. Some studies in the past have focused on studying coastal *SST* trends, recognizing that not all coastal regions show the same patterns as the open ocean. It was identified that regional differences in the coastal warming rate could be explained by local and remote forcing factors, such as the wind regime, freshwater inputs, upwelling events, and thermohaline circulation (Prigent et al., 2020; Santos et al., 2011). For example, Varela et al. (2018) found that upwelling depresses heating rates regardless of the region being considered. Opposite trends in *SST* can even be obtained when considering different spatial scales or temporal periods (Santos et al., 2011). Even though coastal or regional analyses focused on changes in *SST* seasonality are scarce, some studies have been conducted globally. Jo et al. (2022) predicted that the global seasonal cycle of *SST* will have an amplitude increase of 30 % ± 20 % until the end of 21st century. Through a global analysis, Lima and Wethey (2012) found that 46 % (38 %) of the coastline has experienced a significant decrease (increase) in the frequency of extremely cold days (hot days) and that the onset of the warm season is advancing significantly earlier in the year in 36 % of the temperate coastal regions.

Despite this research base, more evidence and understanding of coastal changes in *SST* under a warming climate is needed (Xu et al., 2021). This is particularly the case for the Western Iberian Coast, the focus area of this paper. The Western Iberian Coast is an internationally relevant region from a social and economic perspective, which is still underexplored regarding the quantification and characterization of *SST* changes. Although projections suggest increasing trends in *SST* in the region, only a few studies have provided long-term evidence to support this (*e.g.*, Santos et al., 2011; Santos et al., 2012; Varela et al., 2018). Varela et al. (2018) framed the Iberian Coast as an upwelling region with depressed heating rates. However, to our knowledge, there is no available long-term assessment of *SST* variability with the resolution to allow a regionalized analysis of the Iberian Coast that directly relates the observed variations to atmospheric data and climate teleconnections. Moreover, there is currently still little information available about changes in the timing of *SST* maximums/minimums or in their variability for the Western Iberian Coast. The lack of recent studies focusing on changes on the seasonality of *SST* represent a relevant knowledge gap. Therefore, the overall aim of this paper is to quantify changes in *SST* along the Western Iberian Coast over the past four decades. The objectives of this analysis are to: (1) determine variations in the seasonality of *SST*, by assessing changes in amplitude, maxima and minima, the timing of the maxima and minima and in the number of days where *SST* is above average; (2) quantify long-term *SST* trends and assess if these vary spatially along the coast; and (3) examine the main drivers of the observed *SST* changes, integrating atmospheric datasets and different climate teleconnections. We consider the longest Portuguese *in situ* datasets available and long-term observations gathered along the Spanish coast. These datasets were also used to validate the quality of *SST* satellite data retrievals that were used to obtain a more complete temporal and spatial coverage of the study area.

1.1. Western Iberian Coast

The Iberian Peninsula is located at the most southwesterly point of Europe, with the Atlantic Ocean bordering it to the west (Fig. 1). Its western area encompasses mainland Portugal and Galicia, an autonomous region of Spain. According to the Köppen climate types, the Western Iberia has a Mediterranean climate with warm/hot summers (Santos et al., 2023), From Cape Espichel northwards, Portugal presents a shelf 20–50 km wide and a continental slope from 6 % to over 20 %. Southwards, the shelf is narrower, 10–20 km wide and a continental slope of about 4 % (Fortunato et al., 2002) (Fig. 1).

The territory is part of the Eastern North Atlantic Boundary system (Mantas et al., 2019) and during spring and summer (April/May–September/October), it is characterized by northerly jet stream winds that force a longshore equatorward jet that transports cold and nutrient rich upwelled water (Relvas et al., 2007). About a month after the northerly winds become predominant, cold water filaments begin to develop associated to offshore currents of up to 0.5 m/s. These filaments can often extend >200 km offshore (Relvas et al., 2007). In contrast, during the winter, westerly and southerly winds prevail, originating a surface current that transports warmer and saltier waters to the north, known as the Iberian Poleward Current (IPC) (Relvas et al., 2007; Teles-Machado et al., 2015; Sousa et al., 2017). Please see Peliz et al. (2005), Criado-Aldeanueva et al. (2009) and García-Lafuente et al. (2006) for detailed information about the circulation regime along the Western Iberian Coast and the south of Portugal.

2. Data and methods

2.1. Sea surface temperature (SST)

Two different sources of *SST* were used, *in situ* and satellite-derived, and these are described in detail below.

In situ SST observations were collected using coastal oceanographic buoys managed by the *Instituto Hidrográfico* (Portugal, https://www.hidrografico.pt) and *Puertos del Estado* (Spain, https://www.puertos.es). The data collection process, treatment and subsequent distribution was

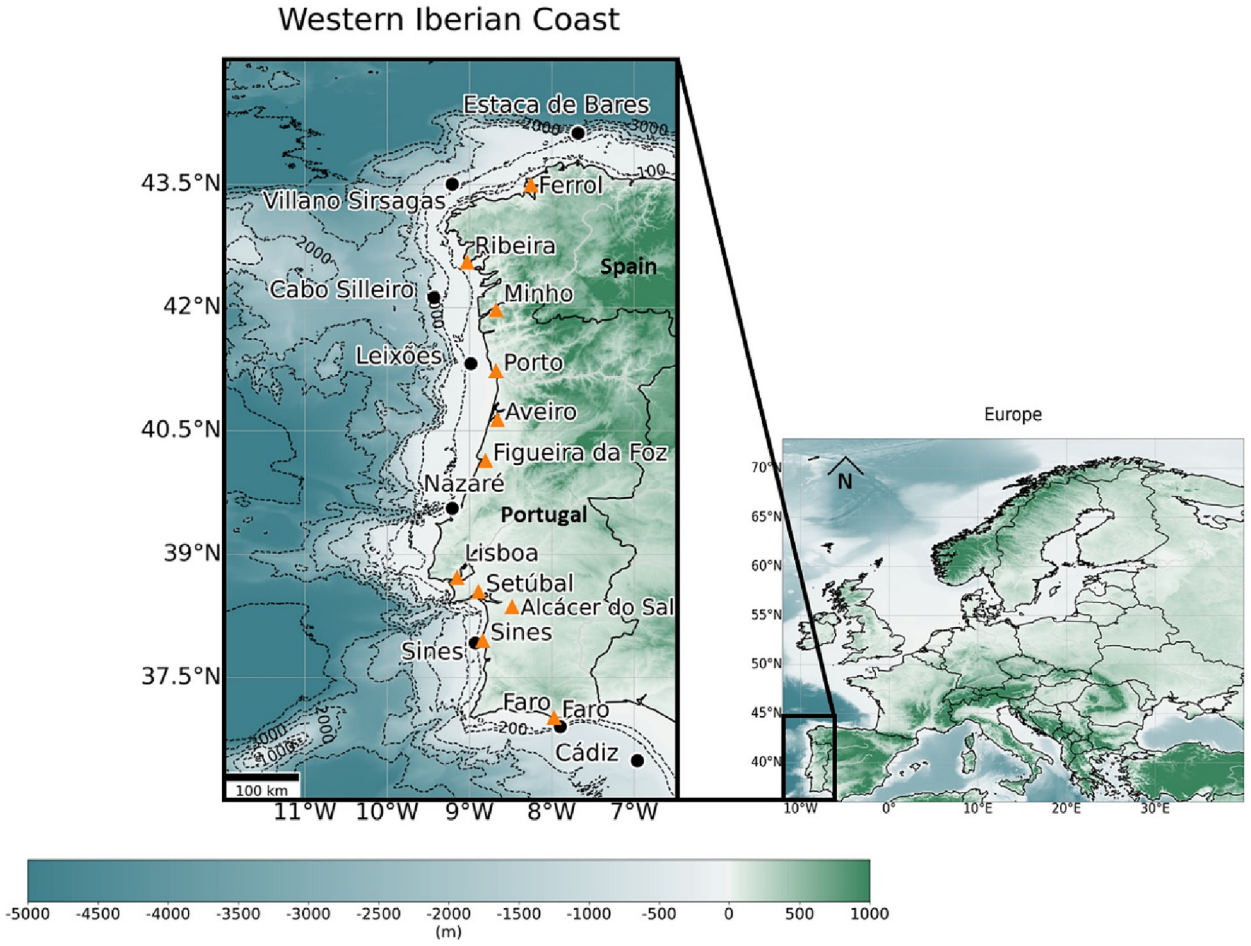

Fig. 1. Representation of the Western Iberian Coast and its context in the European continent. Coloring and contour lines represent the bathymetry (blues) and the topography (greens) of the region in meters. Major rivers are represented in light grey. The oceanographic and meteorological stations considered are also represented in black dots and orange triangles, respectively. Bathymetry and topography data source: GEBCO Compilation Group (2022) GEBCO 2022 Grid (doi:https://doi.org/10.5285/e0f0bb80-ab44-2739-e053-6c86abc0289c).

carried out by these institutions, who kindly provided their datasets for this study. The station names and locations are shown in Fig. 1 and listed in Table 1. The duration of the datasets is also listed in Table 1. The earliest record is at Faro and covers the period 1986–1992 and 2000–2020. Originally, the time series had an hourly temporal resolution but daily averages were calculated and used in this analysis.

Given the lack of longer time series of *in situ* data, to expand the temporal and spatial coverage of this study, satellite remote sensing products were used. Three products were tested to see which one was most suitable for the analysis. The first was a product which provides daily estimates of global *SST* depth (≈20 cm) based on observations from multiple satellite sensors, produced by the ESA Climate Change Initiative (CCI) and the *SST* CCI project (Good et al., 2019; Merchant et al., 2019). The level-4 *SST* dataset with a spatial resolution of 0.05° was used, covering the period from the 1st of January 1982 to the 31st of December 2021. The second was a GHR*SST* MUR product, a Level-4 *SST* dataset provided by the JPL Physical Oceanography DAAC using wavelets as base functions in an optimal interpolation approach on a global 0.01° grid (Chin et al., 2017; JPL MUR MEaSUREs Project , 2015). The dataset has a daily coverage since the 1st of June 2002. For the purpose of this analysis, only data until the 31st of December 2021 was considered. The third was a ERA5 product, the fifth generation ECMWF reanalysis for the global climate and weather (Hersbach et al., 2018). The *SST* dataset was used from the 1st of January 1979 to the 31st of December 2021. The product also has a daily temporal resolution with a spatial resolution of 0.25°.

Table 1
Designation, location and temporal coverage of the oceanographic stations.

Oceanographic stations	Responsible institution	Latitude (° N)	Longitude (° W)	Temporal coverage of dataset
Estaca de Bares	Puertos del Estado (Spain)	44.12	7.68	2001–2021
Villano Sirsagas	Puertos del Estado (Spain)	43.50	9.21	2001–2021
Cabo Silleiro	Puertos del Estado (Spain)	42.12	9.43	2001–2021
Leixões	Instituto Hidrográfico (Portugal)	41.32	8.98	1998–2021
Nazaré	Instituto Hidrográfico (Portugal)	39.56	9.21	2010–2021
Sines	Instituto Hidrográfico (Portugal)	37.92	8.93	1996–2021
Faro	Instituto Hidrográfico (Portugal)	36.90	7.90	1986–1992; 2000–2020
Cádiz	Instituto Hidrográfico (Portugal)	36.49	6.96	2002–2021

Validation of *SST* remote sensing products were performed using coincident *in situ* observations (nearest neighbor, single pixel matchup analysis). Several statistical tools were used, as described in Sent et al. (2021), including: (i) linear regression parameters, with the coefficient of determination (R^2), and the slope and intercept; (ii) root mean square error (*RMSE*); and (iii) bias (*BIAS*). The results of the comparison are given in the Supplementary Materials (Figs. S1 and S2). The *SST* product provided by CCI was considered the one with the best agreement with the *in situ* observations for the Western Iberian Coast ($R^2 > 0.89$; $RMSE < 0.45$; $BIAS < 0.40$). Therefore, this was the product selected for all *SST* analysis in this study.

2.2. Atmospheric data

Atmospheric *in situ* time series of air temperature, *u* and *v* wind components (horizontal and vertical components, respectively) and total precipitation were provided by *Instituto Português do Mar e da Atmosfera* (IPMA, https://www.ipma.pt/pt/index.html) for 9 stations distributed along the Portuguese coast. Two meteorological stations from the Galician coast were also considered (Ferrol and Ribeira), with historical data provided by MeteoGalicia (https://www.meteogalicia.gal/web/inicio.action). These hourly atmospheric time series were converted into daily averages. The locations of these stations are shown in Fig. 1 and are described in Table S1 in the Supplementary Materials.

ERA5 was also used to complement the *in situ* atmospheric data. From this product, surface temperature (measured at 2 m), *u* and *v*-components of wind (measured at 10 m) and total precipitation were used. The quality of this data was tested in a single-pixel matchup-analysis (supplementary materials, Figs. S3-S6) as described in Sub-section 2.2. After validation, the data was used for further analysis. The Upwelling Index (*UI*) was calculated following the equations described in Ferreira et al. (2022) using the ERA5 *u* and *v*-components of wind. Positive values indicate favorable conditions for the occurrence of upwelling.

ERA5 net shortwave radiation (*SWnet*), net longwave radiation (*LWnet*), latent heat flux (*Qlat*) and sensible heat flux (*Qsen*) data was used for a net surface heat flux (*Qnet*) analysis. Net heat flux was calculated following the formulation $Qnet = SWnet + LWnet + Qlat + Qsen$ (Hu et al., 2020), assuming downwards fluxes (into the ocean) as positive, according to the ECMWF convention.

2.3. Methods

2.3.1. Analysis of SST seasonality variations

To quantify variations in the seasonality of the *SST* along the Western Iberian Coast, the whole period of the CCI dataset (1982–2021) was considered. For comparison purposes, this analysis was also conducted for air temperature using the ERA5 dataset. The variability of the following parameters was assessed in a trend analysis: (i) Amplitude; (ii) Maximum and minimum monthly values; (iii) Week of occurrence of the maximum and minimum values; and (iv) Number of days above average and timing of the first day above average. The amplitude was calculated considering monthly means and the difference in °C between the maximum and minimum values of each year. The monthly maximums/minimums obtained for each year were calculated in order to evaluate inter-annual variability. For each year, the week of the year in which the maximum/minimum value was observed (considering weekly averages) was determined, with the purpose to identify if trends of delays or advances of these moments had occurred within the studied period. The number of days per year with *SST* above the average of the whole time series was calculated; likewise, the first day of the year above that average was identified for each year of the time series.

2.3.2. SST time series analysis

To avoid interpreting natural variability as part of the trends, the seasonality of all the time series (*in situ*, CCI and ERA5 datasets of *SST*, atmospheric data and *UI*) was first removed. 5-year average seasonal cycles with daily resolution were calculated, using a moving average approach. This period was chosen, as it allowed the removal of the intra-annual variability as well as inter-annual changes in seasonality. All trends were determined using linear regressions and their significance was assessed considering *p*-values lower than 0.05 (*i.e.*, 95 % confidence). Simple linear regression analysis is one of the most widely used trend detection tests worldwide (Meshram et al., 2017; Singh et al., 2021). CCI trend analysis was focused on the period between 1984 and 2019 while ERA5 trends were considered for the years 1981 to 2019.

To study the occurrence of changes along the *SST* series, the Pettitt test was applied to the CCI datasets. The Pettitt test is a nonparametric method (rank-based and distribution-free test), widely used on hydrometeorological variables, to determine the occurrence and timing of abrupt and significant changes in the mean of a time series (Li et al., 2014; Serinaldi and Kilsby, 2016). Following Pettitt's test, a series of dataset Y_1, Y_2, …, Y_n, has a change-point at "n" such that Y_1, Y_2,.., Y_n has a distribution function F1(y) that is dissimilar from the distribution function F2(y) of the subsequent portion of the sequence y_{n-1}, y_{n-2}, y_{n-3} …, y_n (Getahun et al., 2021).

To better understand the interannual and spatial variability of *SST* and the results of the Pettitt test, the annual and monthly anomalies of *SST* were determined by calculating the difference between the mean value of a specific year/month and the climatological mean of the time series.

2.3.3. Main drivers of SST changes

To investigate the main drivers of *SST*, the correlations between the daily *SST* and the atmospheric timeseries were calculated. Similarly, annual *SST* anomalies were correlated with the annual averages of the different atmospheric variables. To allow the comparison of the products, the ERA5 spatial grid was converted to the spatial resolution of CCI, through an interpolation using the nearest neighbor method.

Additionally, time series of North Atlantic Oscillation (*NAO*) (https://www.ncei.noaa. gov/access/monitoring/*NAO*/), East Atlantic teleconnection pattern (*EA*) (https://www.cpc.ncep. noaa.gov/data/teledoc/ea.shtml), Atlantic Multidecadal Oscillation (*AMO*) (https://psl.noaa.gov/data /timeseries/AMO/; smoothed version), Southern Oscillation Index (*SOI*) (https://www.ncei.noaa. gov/access/monitoring/enso/soi#calculation-of-soi) and Western Mediterranean Oscillation Index (*WeMOI*) (https://crudata.uea.ac.uk/cru/data/moi/) were also considered as potential drivers of the *SST* changes. These time series presented monthly averages that were interpolated to daily data or averaged to annual values, to allow the comparison with the CCI *SST* time series or the *SST* annual anomalies, respectively. *NAO* was chosen as is the leading mode of atmospheric variability in the North Atlantic-European sector (Dalelane and Wetterdienst, 2019; Jing et al., 2019). Similarly, *EA* was studied as it is the second most prominent mode of low-frequency variability over the North Atlantic. It has a similar structure to that of *NAO* and plays an important role in regulating weather along Europe (Krichak and Alpert, 2005; NOAA, 2012). *AMO* forces long-term temperature changes that affects the North Atlantic ocean-atmosphere interactions, with cooling and warming phases every 50–80 years (Knight et al., 2006; NOAA/ESRL , 2022). *SOI* is an indicator of the development and intensity of El Niño and La Niña events in the Pacific Ocean, which was selected for the present analysis as it has been observed to sometimes influence *SST* in some areas of North Atlantic (Commonwealth of Australia, 2022; Jiang and Zhang, 2022). *WeMOI* was chosen as it is the teleconnection with the strongest effects on the climate variability over the eastern Iberian Peninsula, when compared with the *NAO* or the *AMO* (Lana et al., 2016).

3. Results

3.1. Changes in the seasonality of SST

Maps with the linear trend of the amplitude and the maxima and minima are shown in Fig. 2a, b and c, respectively. Only grid cells with statistically significant trends (95 % confidence interval) are colored. As is evident

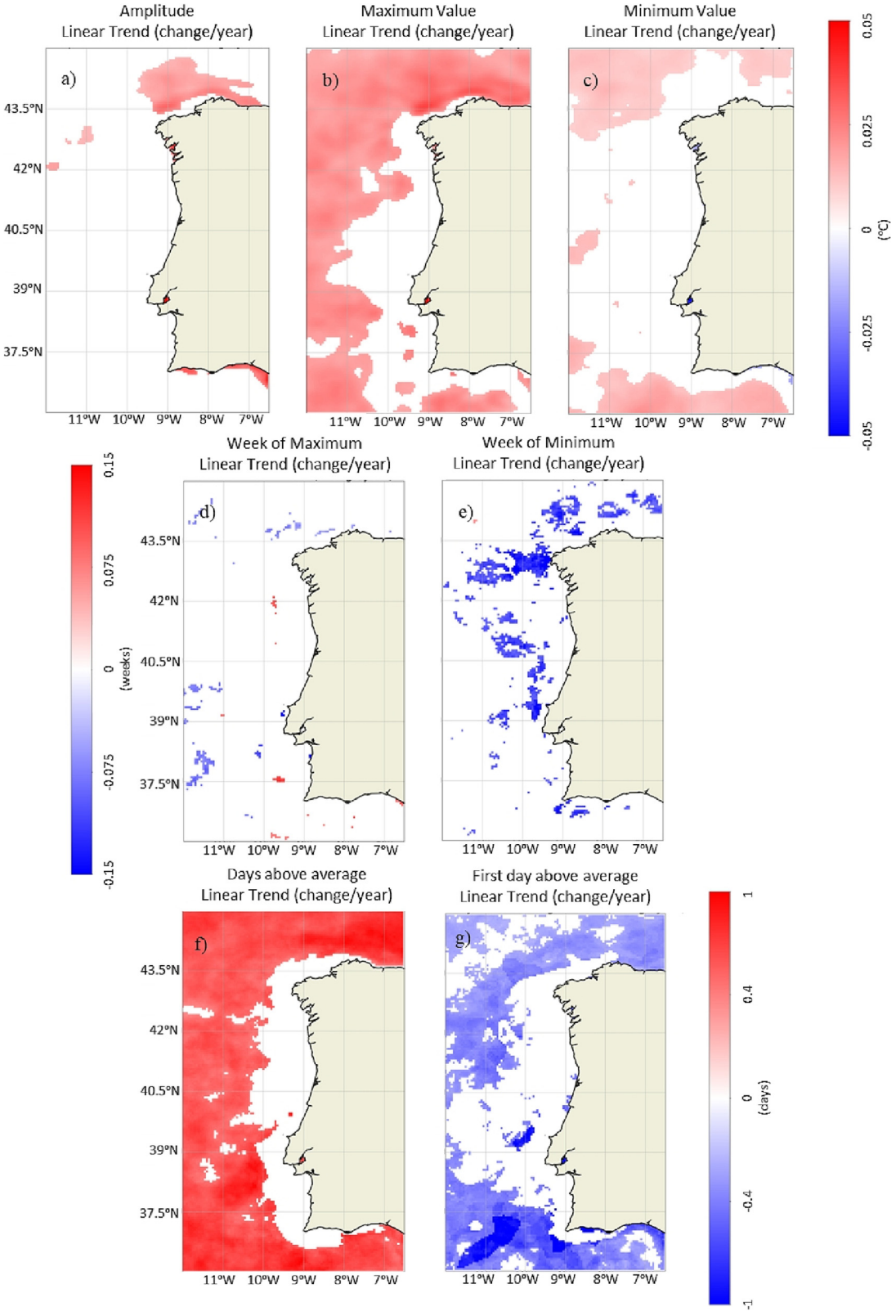

Fig. 2. Change in the seasonal patterns from CCI SST between 1982 and 2021. Significant trends (95 % confidence interval) are presented for changes in: a) amplitude; b and c) the maximum and minimum monthly values; d and e) the week of occurrence of the maximum and minimum values (weekly averages); f) the number of days above average; g) the occurrence of the first day above average.

in Fig. 2b, an increase between 0.025 and 0.050 °C/year was observed in the annual maximum of *SST* off the coast of Western Iberia. However, significant trends were not observed along the coastal strip. For most of Western Iberia, the variation in the annual minimum of *SST*, shown in Fig. 2c, was not statistically significant. However, an increasing trend was seen in the northern and southern region of the peninsula. No significant

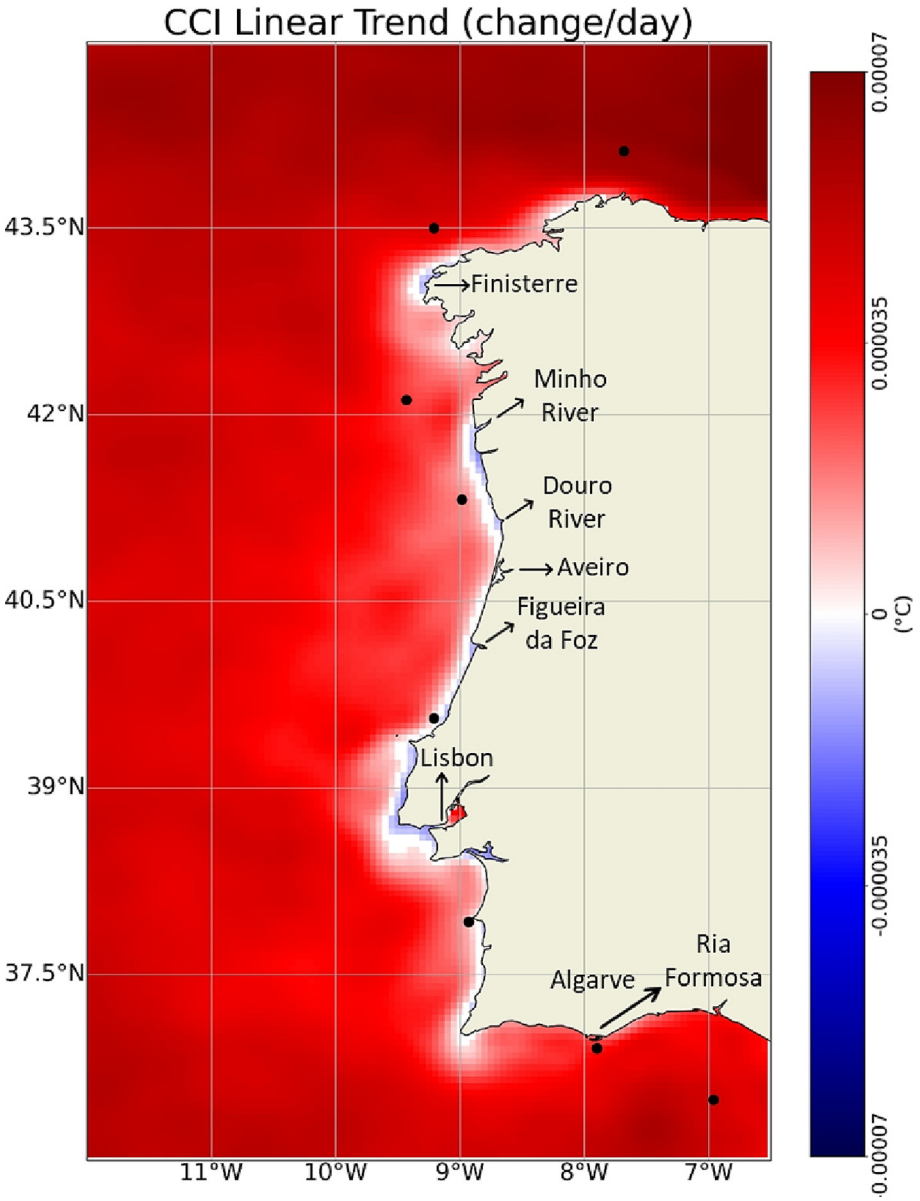

Fig. 3. Sea surface temperature trends from CCI, after a seasonality removal. Time coverage between 1984 and 2019. Only significant trends (95 % confidence interval) are presented. The black points represent the location of the *in situ* buoys.

changes in the amplitude of the *SST* were observed in the studied region, as shown in Fig. 2a. A significant increase in the amplitude was only seen on the northern coast of Galicia and along the Algarve (south) shore.

The linear trend of the timing of *SST* maxima and minima is mapped in Fig. 2d and e, respectively. As it is possible to see in Fig. 2d, the minimum annual value (considering weekly averages) is currently tending to occur by about 0.15 weeks/year (1 day/year) earlier than in the beginning of the period of study, mainly along the coast of Galicia, but with some dispersion. No significant patterns of anticipation or delay in the timing of the maximum annual values were observed, as shown in Fig. 2d.

Lastly, Fig. 2f and g shows the trend of the number of days per year in which the *SST* was above the average and the trend of the first day of the year with that characteristic, respectively. The number of days above the average increased outside the coastal region (Fig. 2f). Similarly, the first day of the year where the *SST* exceeded the average appeared early regarding the beginning of the studied period, in some regions about 1.5 days/year, as it is possible to see in Fig. 2g.

Comparatively, the same analysis was performed for air temperature, and the changes in seasonality were much less evident, as shown in Fig. S9 in Supplementary Materials. A significant increase in the value of the annual maximum has been observed, but only over the southeastern region of Portugal and over the Galician coastal ocean. For air temperature, the timing of the annual maximum presented a significant trend to appear earlier in the order of 1.5 weeks/year (1 day/year), mainly over a large part of the mainland.

The strongest trends of increase in the number of days per year on which the air temperature was above average were observed over the Alentejo and Algarve regions. Over the coastal ocean this pattern was not so strong and only showed significant variations at offshore locations, almost 200 km from the coast (except on the southern margin of the peninsula) (Supplementary Materials, Fig. S9).

3.2. Long-term trends of SST and their spatial variability

A map with the results of the trend analysis is presented in Fig. 3. *SST* has been increasing in the past decades, as shown in Fig. 3. This increase is generalized to the coastal oceanic region, but its magnitude differs locally. The magnitude of the trend increased with distance from the coast

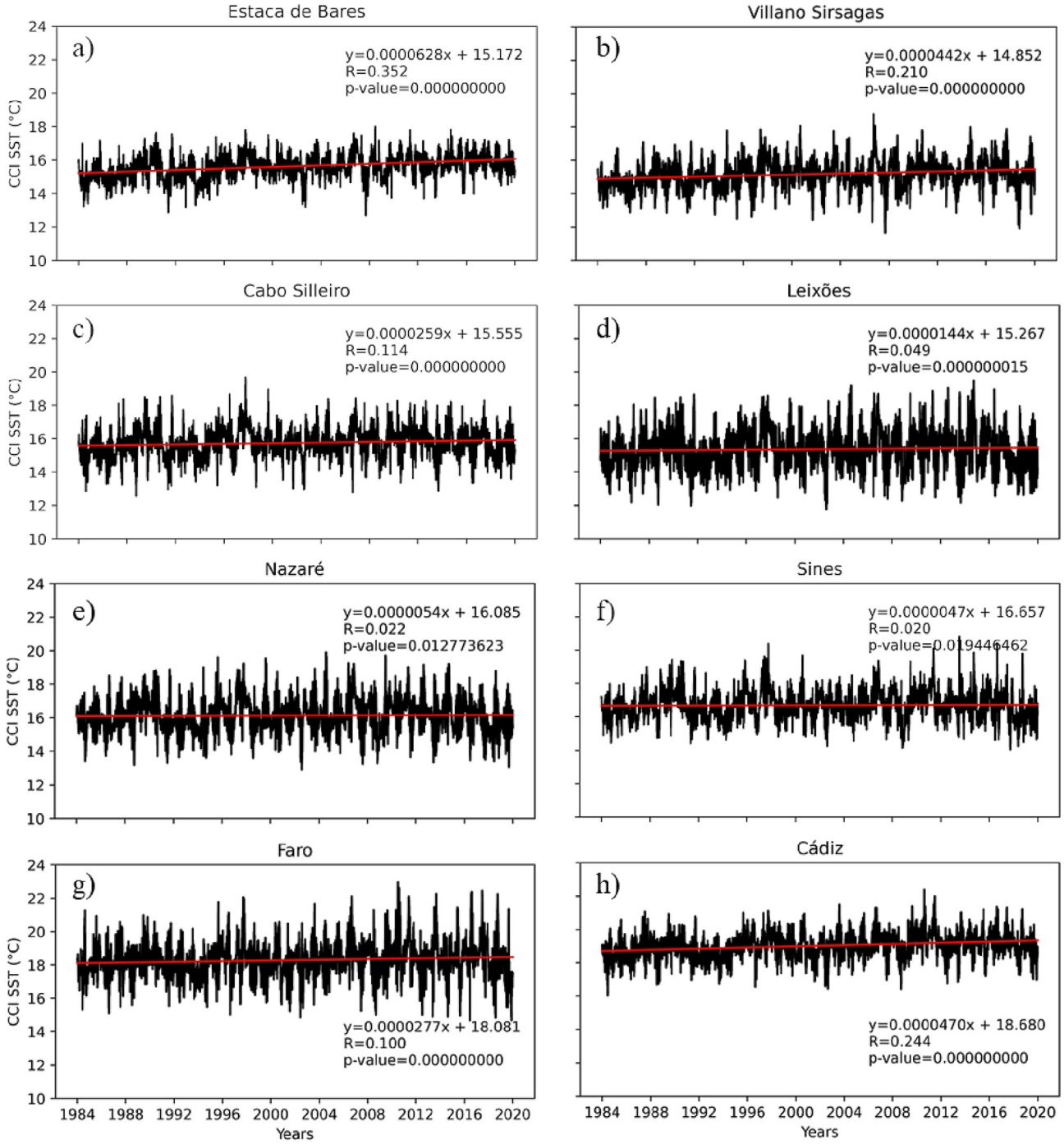

Fig. 4. Trend analysis of the CCI time series from the *in situ* sampling stations, after a seasonality removal. Temporal coverage between 1984 and 2019. The coefficient of correlation (R) and significance of the trends (p-value<0.05) are also presented.

(Fig. 3). About 200 km from the west coastline, an increase of nearly 0.000044 °C/day (0.16 °C/decade) was observed. The North and South margins of the Peninsula showed the strongest trends, with the North coast achieving an increase of 0.000063 °C/day (0.23 °C per decade). Fig. 4 presents the CCI time series extracted from the *in situ* stations, with the respective trend analysis, whose results are listed in Table 2.

Despite the generalized increase, decreasing trends in the *SST* were also observed near the coastline, as shown in Fig. 3 (spatial average ≈ -0.000014 °C/day; −0.05 °C/decade). This pattern mainly covered the region of Finisterre (Galicia) and the continental margin between the following sections: i) Minho to Douro; ii) Figueira da Foz to Lisbon. It should be noted that the coastline on the southern margin of the peninsula showed positive trends throughout its area.

To quantify the evolution of the *SST* trends and understand whether they have accelerated or decelerated in recent years, the trend assessment was repeated only considering decadal periods. Maps of the *SST* trends obtained between 1990 and 1999, 2000–2009 and 2010–2019 are shown in Fig. 5a, b and c, respectively. The increasing trends observed over the whole period have been weakening along the coast in the last 3 decades, as shown in Fig. 5. Moreover, the patterns have reversed, and significant decreasing trends were observed in almost the entire Iberian coastal region over the last 10 years (Fig. 5c). Whereas between 2000 and 2009, only

Table 2
Sea surface temperature trends (change per day and change per decade) between 1984 and 2019 in the location of the sampling stations from the CCI dataset (without seasonality).

Stations	Change/day (°C)	Change/decade (°C)
Estaca de Bares	0.0000628	0.223
Villano Sirsagas	0.0000442	0.161
Cabo Silleiro	0.0000259	0.095
Leixões	0.0000144	0.053
Nazaré	0.0000054	0.020
Sines	0.0000047	0.017
Faro	0.0000227	0.083
Cádiz	0.0000470	0.172

anomalies were observed along the west shoreline of the peninsula between 2015 and 2019 (Fig. S10). The year with the strongest positive anomalies was 1997.

A map with the results of the Pettitt test is shown in Fig. 7, and it allows us to identify the abrupt changing point in the time series that caused their heterogeneity. Different periods are represented in different colors. For most oceanic waters, the probable significant point of change was observed between 1994 and 1995, as observed in Fig. 7. This period is within the phase of the *AMO* inversion, which went from negative to positive anomaly stage. Near the coastline, a much more recent changing point was observed in 2018. When observing the annual *SST* anomalies (supplementary materials, Fig. S10), 2018 was the year with the strongest and most spatially generalized negative anomalies among the studied period, that mostly affected

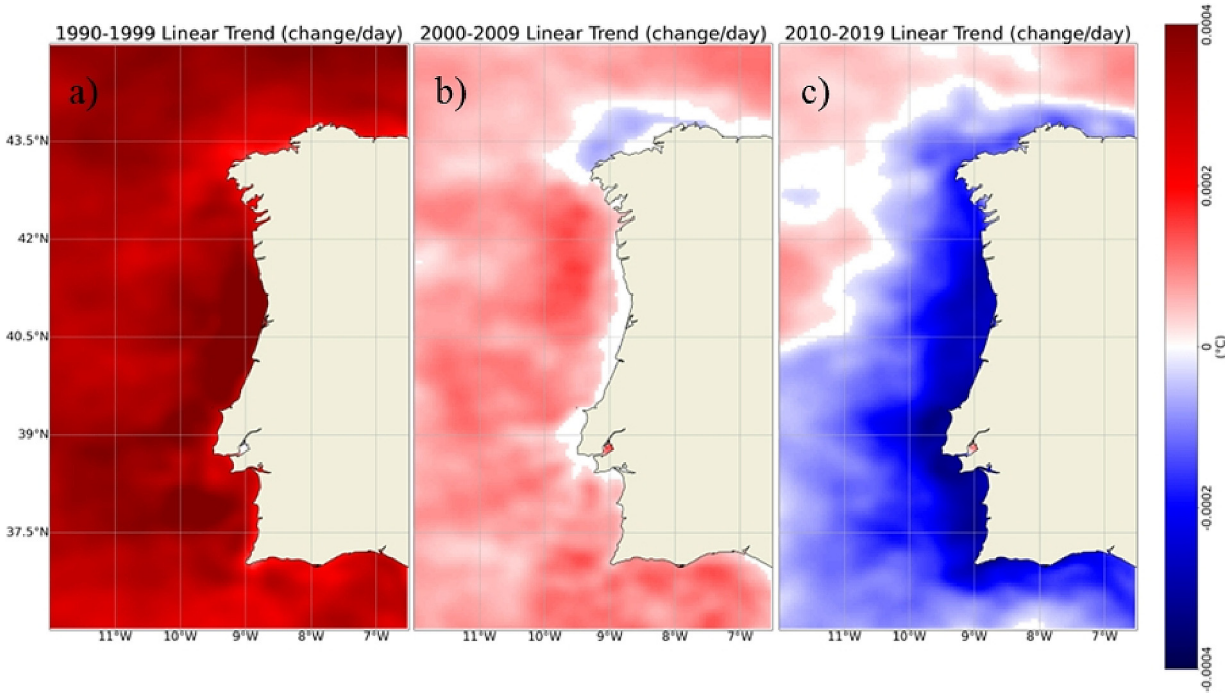

Fig. 5. Sea surface temperature trends from CCI, after a seasonality removal. Time coverage between 1990 and 1999 (a), 2000–2009 (b) and 2010–2019 (c). Only significant trends (95 % confidence interval) are presented.

the Northwest Galician coast showed significant decreasing trends, as it is observed in Fig. 5b.

Monthly anomalies of *SST* between 1984 and 2019 are shown in Fig. 6; years are plotted on the x-axis and months on the y-axis. There was a strong temporal evolution of the spatially averaged *SST* anomalies. Between 1990 and 1999, the Iberian coast went from 5 years with mostly negative anomalies to 5 years of stronger positive anomalies, as observed in Fig. 6, which could suggest an increase in *SST* over the 10 years. This increase was not as pronounced in the following decade, despite the existence of mostly positive anomalies through the period. Between 2010 and 2019, although mostly positive anomalies were observed, the decade ended with an interim of negative anomalies in some months between 2018 and 2019, which has led to the observed downward trends. It also seems that winters got increasingly warmer, as shown in Fig. 6, which corroborates the regional trends of increasing minimum monthly values (Fig. 2).

From the anomalies analysis we see overall positive anomalies from 1995 onwards throughout the area (Fig. 6 and Fig. S10). Negative anomalies were observed in some years and regions near the coast through the period, but framed in a scenario of mostly positive anomalies, as shown in Fig. S10 of the Supplementary Materials. Continuous negative annual the near coastal region. This was also the year with the strongest positive NAO index ever recorded.

3.3. Main drivers of SST changes

Several parameters were considered as potential drivers of the *SST* variations. The mean seasonal cycle of each atmospheric variable, as well as of the *SST,* is illustrated in Fig. 8, to give an insight on the variability of the data. Fig. 8 presents only the most northerly atmospheric station and its closest oceanographic station as an example. The average seasonal cycles of the ERA5 atmospheric variables for all the stations can be found in Supplementary Materials (Figs. S7- S8).

Maps showing the trends of the atmospheric datasets are presented in Fig. 9. Panels a, e, i and m of Fig. 9 consider the whole period of data and the panels b-d, f-h, j-l and n-p consider each one of the last three decades. When considering the whole period analyzed, air temperature increased significantly, as shown in Fig. 9a. This increasing trend was of greater magnitude over land (almost 0.000055 °C/day or 0.2 °C/decade) than over the ocean (≈0.000027 °C/day, 0.1 °C/decade). In contrast, along the coastline, it was almost negligible. For this same period (1981–2019), an increasing

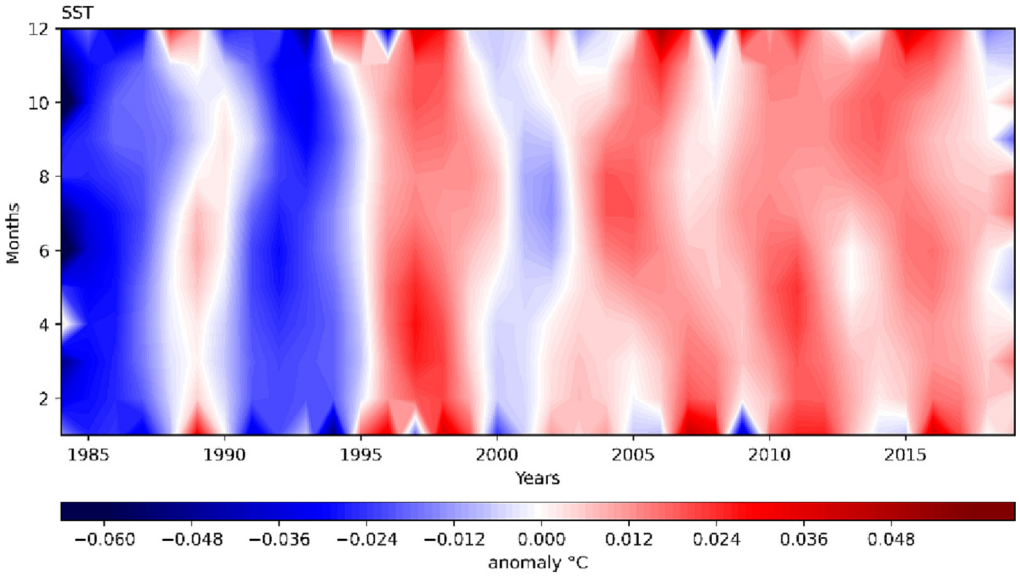

Fig. 6. Monthly anomalies from CCI SST between 1984 and 2019 considering a spatial average of the region.

trend in the *u*-component of the wind was observed for most of the Portuguese mainland and offshore ocean, as seen in Fig. 9e. Similarly, also the wind *v*-component increased mainly over the central and southern Portugal and the adjacent ocean (Fig. 9j). This indicates an increase in the frequency and intensity of winds from the West and North in the past decades. These wind patterns promoted an intensification of the upwelling

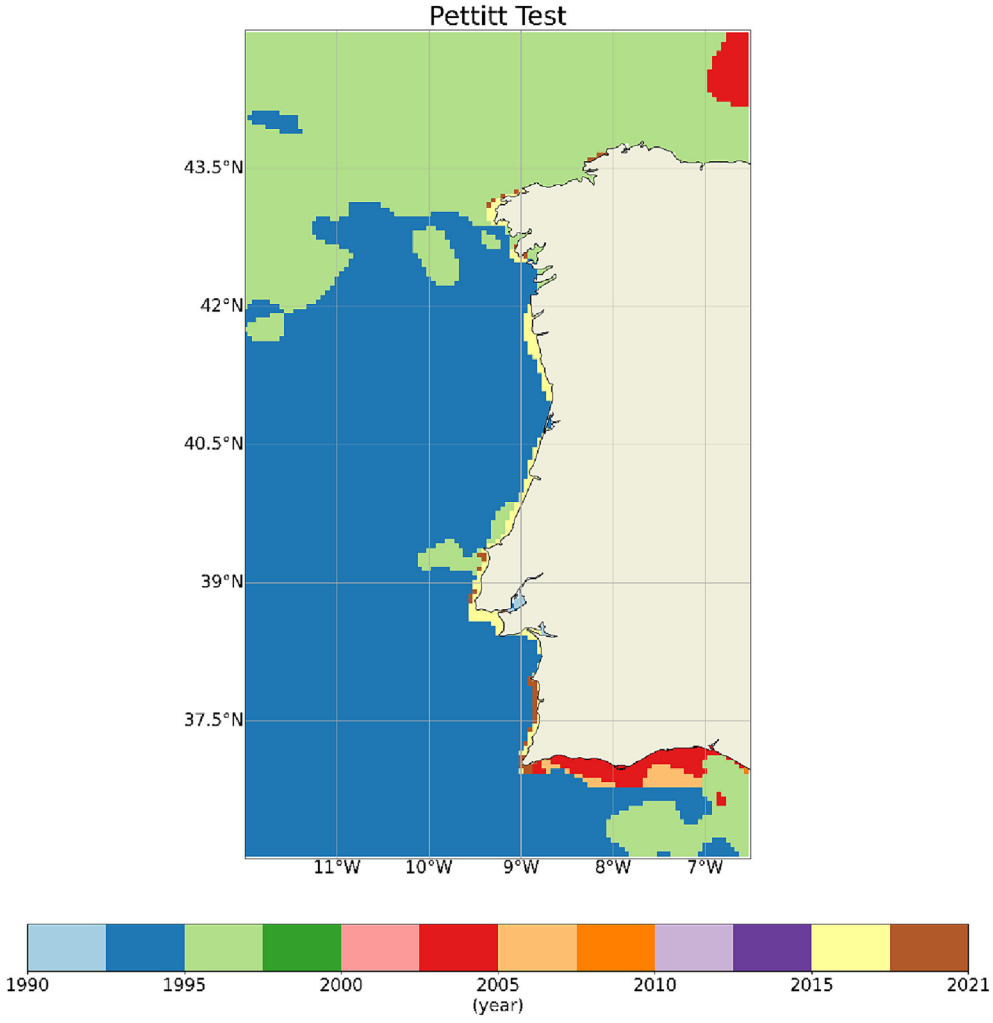

Fig. 7. Significant probable changing point of the CCI time series along the Western Iberian Coast, based on Pettitt tests. Temporal coverage between 1984 and 2019.

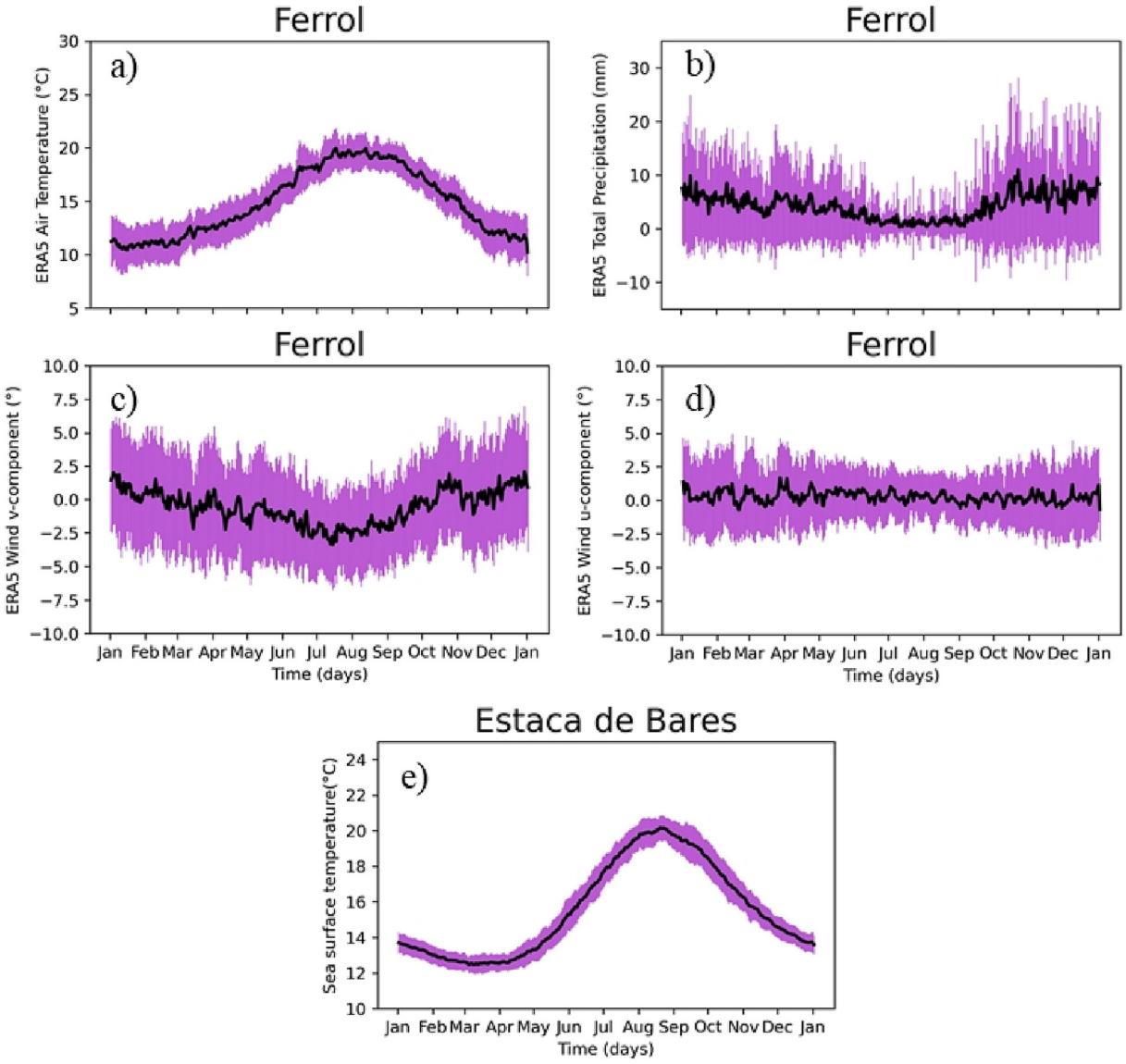

Fig. 8. Mean seasonal cycle of air temperature, total precipitation and wind u and v-components of ERA5 data between 1979 and 2021, for the location of Ferrol *in situ* sampling stations. SST mean seasonal cycle of CCI data between 1982 and 2021, for the location of Estaca de Bares *in situ* station, the closest one to Ferrol. Standard deviation colored in purple.

index in part of the Northern region of Galicia and along the Portuguese west coast from Aveiro southwards, as shown in Fig. 9n. No significant trends in total precipitation were observed either over the mainland or the coastal ocean (data not shown).

Considering the last 3 decades separately, all atmospheric variables showed higher magnitude trends in the last decade than when considering the whole period, as observed in Fig. 9d, h, l and p, albeit with some local differentiation. In the case of air temperature, significant decreasing trends were obtained along the coast between 2010 and 2019 (Fig. 9d), which match the decreasing trends detected for *SST*. On the other hand, Fig. 9d also shows that between 2010 and 2019, air temperature increases of around 0.05 °C/year were simultaneously observed over land. The decreasing *SST* temperatures recorded in the Finisterre zone between 2000 and 2009 corresponded to an increase in Northerly winds in that region during that period.

To further clarify the drivers of the *SST* trends obtained, maps showing correlations between the *SST* annual anomalies and the different atmospheric variables and indices are presented in Fig. 10. Once more, only significant correlations are colored (95 % confidence interval). The variation in air temperature appeared to strongly justify the *SST* anomalies observed throughout the region, as observed in Fig. 10a. Also, positive correlations were observed between *SST* anomalies and mean annual precipitation in the coastal region between Aveiro and Ria Formosa, showing that positive values of *SST* anomalies were indirectly associated with higher values of precipitation in that region (Fig. 10b). The *NAO* index has also influenced the *SST*, as shown in Fig. 10f, with negative correlations mainly in the southwest region of the Peninsula. Near the coast, there was no significant relationship between the two variables. The teleconnection that presented the highest correlation with the *SST* anomalies was the *WeMOI* (mean R = -0.47; stronger correlation along the coast of the Algarve, $R \approx 0.70$), as shown in Fig. 9j. However, this correlation was not observed in two areas of the Galician coastal zone. The *EA* was shown in Fig. 10i to be not responsible, at least directly, for the *SST* anomalies observed near the coast.

Wind *v*-component was very relevant in driving *SST* variations along the coastal region, with positive correlations extending to about 200 km in front of Lisbon, as observed in Fig. 10c. This shows that stronger negative *SST* anomalies, particularly at the coast, were associated with stronger Northerly winds. The only part of the coastline that showed no correlation with the wind *v*-component was the north margin of Galicia. Conversely to the *v*-component of wind, only the south margin of the peninsula showed a

significant correlation with the *u*-component of wind, as observed in Fig. 10d, relating higher negative *SST* anomalies with stronger winds form west. As expected, the *UI* clearly relates with the *SST* anomaly patterns obtained from the correlation with the wind components (Fig. 10k). Wind speed presented significant correlations with the *SST* anomalies, mainly along the west coast of the studied region, as shown in Fig. 10e. Both the *AMO* and the *SOI* did not show any patterns of significant relationships with the *SST* anomalies, which suggest that they do not drive any of the seen variation (Fig. 10g and h). The correlation between the daily *SST* data and the different variables, as well as the daily *SST* and the temporal evolution of the spatially averaged anomalies of the different atmospheric variables, can be found in Supplementary Materials, Figs. S11 and S12.

4. Discussion

The present study quantified changes in *SST* over the last four decades by evaluating changes in seasonality, calculating the long-term trends of *SST* and determining the factors that drove those changes. Except in part of the Galician coast, no significant changes in the *SST* amplitude between 1984 and 2019 were observed, which is consistent with the findings of Kessler et al. (2022). Lima and Wethey (2012) showed that the Eastern Atlantic margin has been registering an increase in extreme hot days (8.4 ± 6.6 additional hot days per decade) and a decrease in cold days in the past decades (11.2 ± 7.1 days per decade). The authors found that seasonal warming has been occurring earlier in most of the temperate regions of this

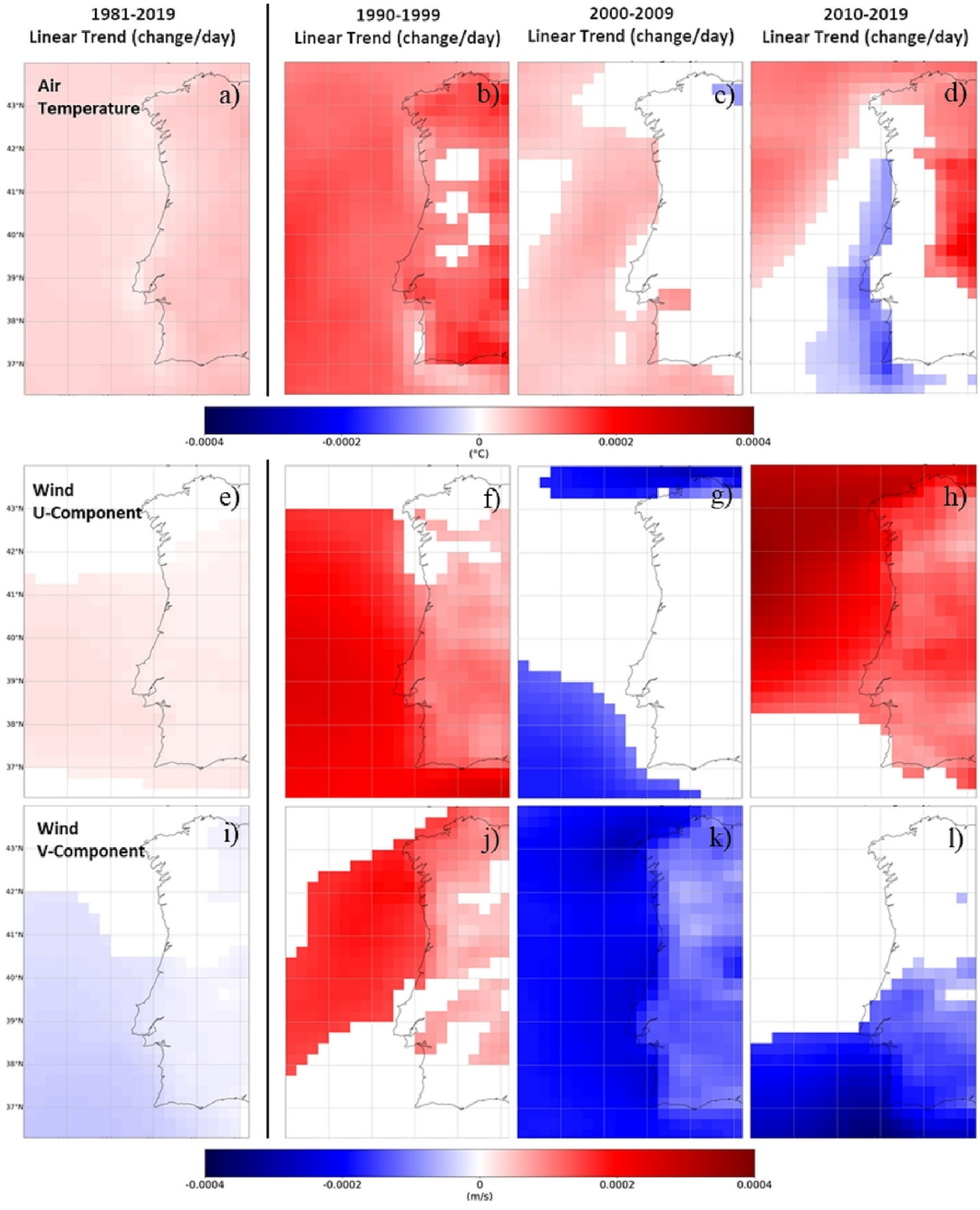

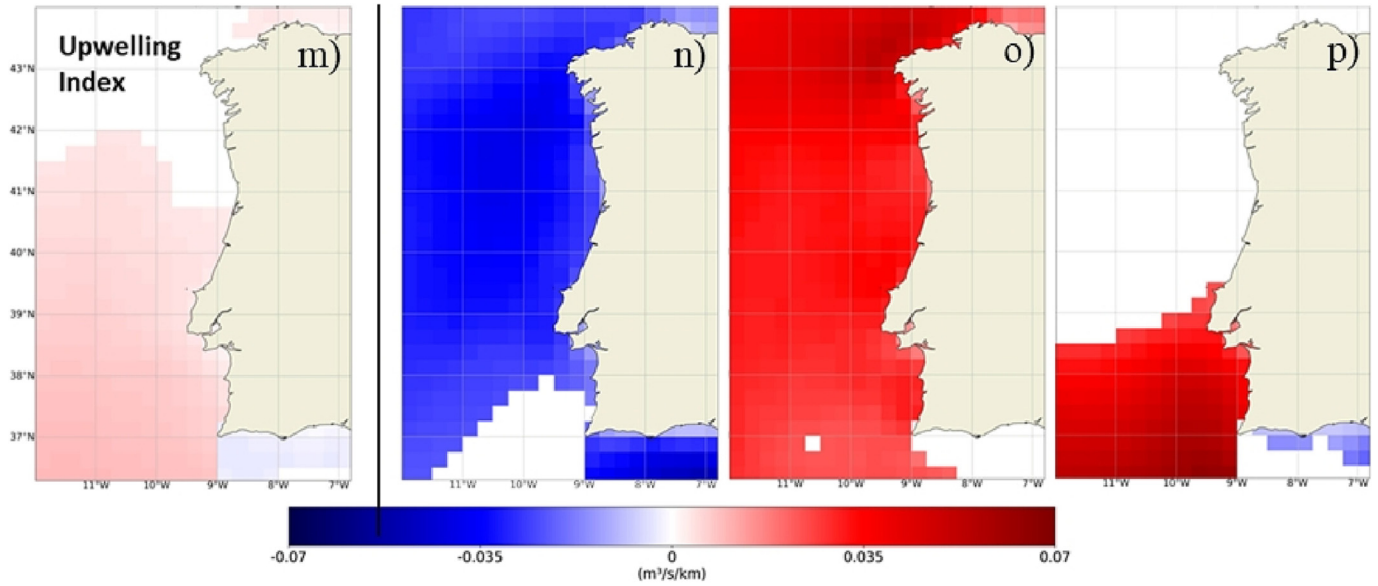

Fig. 9. Air temperature, wind components and upwelling index trends from ERA5, after a seasonality removal. Time coverage between 1981 and 2019, 1990–1999, 2000–2009 and 2010–2019. Only significant trends (95 % confidence interval) are presented.

area, in a rate of 5.6 ± 4.3 days per decade. However, all these changes (yearly frequency of extreme hot and cold days, and average change on the occurrence of seasonal warming) were found to be not significant along the Western Iberian Coast in the study (Lima and Wethey, 2012). Despite the difference in the spatial resolutions considered in that study and in the present study, it was also found here that, overall, the timing of seasonality has not undergone significant changes. On the other hand, we show a significant increase in the number of days per year in which the *SST* was above the average, with an increase rate that fits the average value of Lima and Wethey (2012). The changes in the seasonality of air temperature were much less pronounced than those of *SST*, mainly over the oceanic region. This indicates that the ocean appears to be more sensitive to seasonality changes than the atmosphere at sea level, in the Western Iberian Coastal region.

Any change in the seasonality of *SST* can trigger changes in the seasonal behavior of various living creatures, which in turn affects the functioning of marine ecosystems and human activities dependent on those systems. Seasonality changes should be considered in future projections and examined with climate models (Caputi et al., 2009). Although the ocean seems more susceptible to seasonality changes, for certain regions of the coast, the air temperature showed increasing trends of twice the magnitude of the *SST* trends obtained between 1984 and 2019 (Table S2 of supplementary materials). Moreover, the temperature of the air over land increased almost twice as much as over the ocean and the last decade presented the strongest air temperature trends. This provides further evidence that the ocean has an important climate-regulating effect and works as a more efficient heat absorber than the land, which was supported by our heat flux analysis (Supplementary Materials, Fig. S13) (IPCC, 2019; Hu et al., 2020; Cheng et al., 2021).

Apart from the near-coastal region, the values obtained in the trend analysis are corroborated by those presented by Kessler et al. (2022) and the results of E.U. Copernicus (2022). The increase in *SST* is not uniform worldwide, with the Northeast Atlantic being previously characterized with temperature increases of a lower magnitude than those of the global ocean, between 1960 and 1990 (Casey and Cornillon, 2001). However, we show that, in some regions of the Iberia, namely along the North and Southern margins, higher trends were found than those observed for the northern hemisphere or the global ocean (Hartmann et al., 2013; Wu et al., 2020). The high spatial resolution of the present study provides strong support to the framing of the North coast of Iberia within the "superfast" warming category (>0.21 °C/decade) on the scale of the North Atlantic according to the classification followed by Kessler et al. (2022). As such, this can be considered an at-risk region and, therefore, attention should be focused in assessing the vulnerability of its systems. In the global context however, the trends obtained for the study region are lower than those observed in some of the fastest warming regions, such as the Mediterranean (Pastor et al., 2020; García-Monteiro et al., 2022), the Black (Sakalli and Başusta, 2018), North (Kessler et al., 2022) and the northern Red Seas (Chaidez et al., 2017), the Arabian Gulf (Hereher, 2022) or the Northeast U.S. Continental Shelf (Kessler et al., 2022).

An intensification of the rate of increase in the *SST* near the coast was not observed in the Western Iberian Coast, in contrast to what has been reported for several other regions of the world (Pastor et al., 2020; Wu et al., 2020; Garcia-Soto et al., 2021). In fact, a decrease in *SST* was observed during the last decade, strongest along the shore but still significant up to 200 km from the coast. This decreasing trend was probably caused by abnormal events of recent years, namely the lower *SST* that characterized the year 2018 (Figs. 6 and 7; supplementary materials, Fig. S10). In fact, 2018 had the strongest positive *NAO* index ever recorded (Fig. S1 of supplementary materials). A positive *NAO* leads to a stronger westerly flow into Western Europe and a northward shift of the midlatitude storm track. This causes decreased storminess and below-average precipitation along southern Europe (Visbeck et al., 2001). Westerly winds got stronger in the Western Iberian Coastal region in 2018, with wind velocity also increasing during some months of the year (supplementary materials, Fig. S11). However, it is not possible to conclude that the *NAO* was fully responsible for the observed anomaly, and, to our knowledge, there are not many studies mentioning the common effect of the *NAO* in the *SST* of the southwestern European region to help with that assessment. Moreover, the present analysis showed that the *NAO* did not fully explain the *SST* annual variability near the coastal region of the peninsula.

In fact, our results suggest that the *WeMOI* is more important than the *NAO* in regulating the *SST* variability in this particular region. Therefore, it is possible that the strong negative anomalies obtained in 2018 could have been the result of the combined effect of the *NAO* and the *WeMOI*, that has skewed the last decade's analysis to a decrease in temperature. The decreasing *SST* trends observed near the shore were also probably enhanced by the negative *SST* anomalies observed along the west coast of the peninsula since 2016. An upwelling intensification could possibly justify the observed patterns, as trends point to an increase in the frequency/intensity of these events in the last decades. As seen, upwelling had a significant correlation with negative *SST* anomalies near the coast. During the last

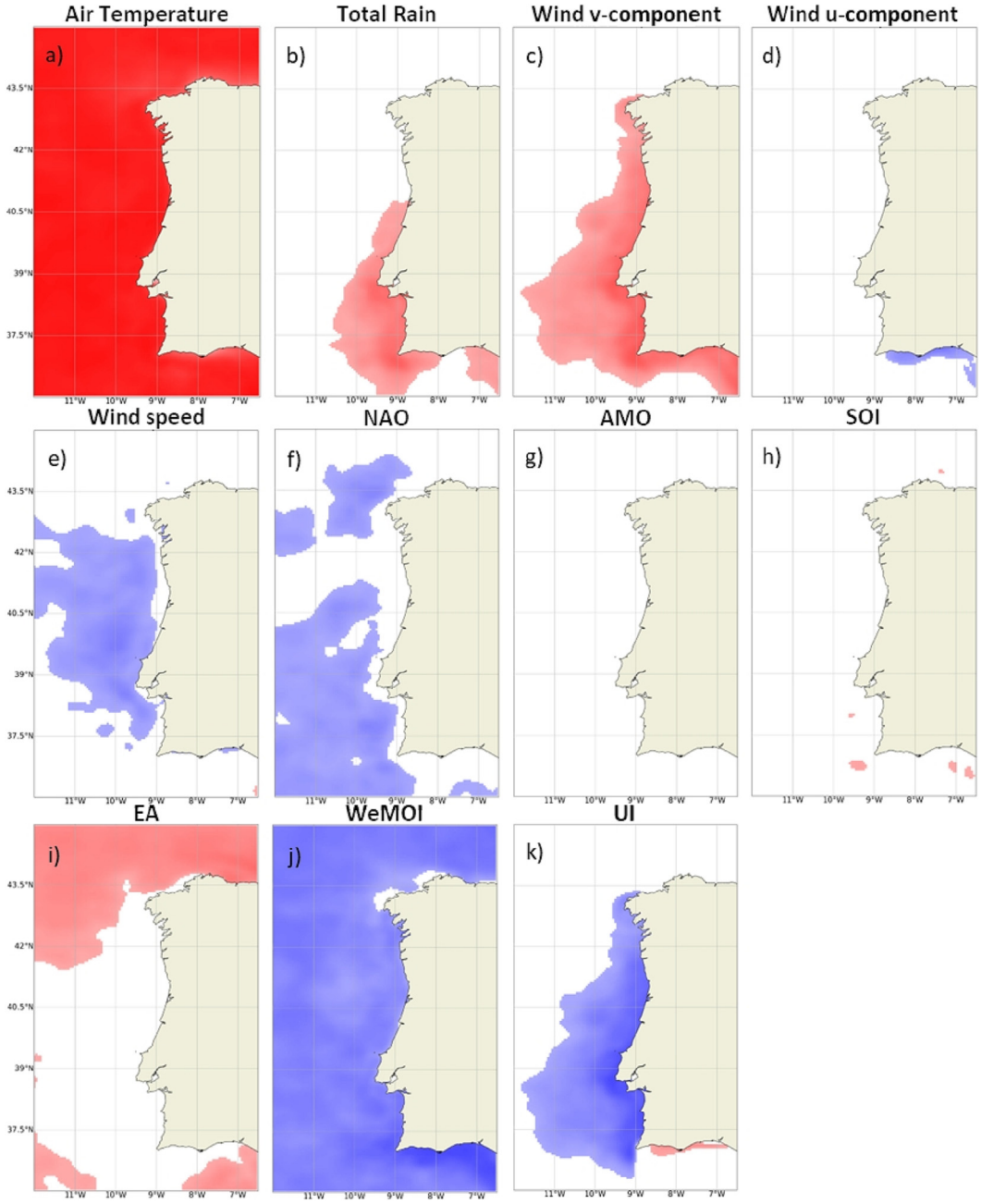

Fig. 10. Correlation coefficients between the CCI SST annual anomalies and annual averages of the different atmospheric variables and teleconnections. Only significant correlations (95 % confidence interval) are presented.

decade, there was also an intensification of the wind intensity increasing trends along the region. Zeng et al. (2019) also detected that wind speed rapidly increased across the globe, particularly in Europe, and justified this change with ocean–atmosphere oscillations, rather than increased surface roughness. The described increase was presented as a rebound of the global downward trend commonly referred to as stilling, that has been observed since the 1980s (Zeng et al., 2019). For the specific case of the Iberian Peninsula, it has previously been reported that the wind stilling ceased since the 2000s (Utrabo-Carazo et al., 2022), which highlights the importance of regional analysis. The authors were not able to explain the cause of this reversal phenomenon, but they hypothesized that it could be linked to the *WeMOI*. The decrease in *SST* observed in the last decade was also observed in the air temperature at the coastline, even though in the rest of the region, air temperature was increasing at its strongest rate. The cause of this air temperature decrease is left unknown and will be the focus of future work.

Air temperature is driving the worldwide rise of mean sea surface temperature (Liu and Yao, 2022), and we find that this is also the case for the Western Iberia. However, we show that the Western Iberian Coast had no significant changes in sea temperature patterns, and identify a weaker *SST* increase than that observed offshore. This suggests that the west coast of the Iberian Peninsula is acting as a buffer for *SST* increase, contrary to the trends observed globally, likely due to the positive trends of upwelling events seen in the latter two decades of the time period (seen in Fig. 9). Upwelling in the Iberian coast has a seasonal occurrence, particularly in the warmer months, and is manifested by a longshore equatorward jet transporting cold and nutrient rich water from the subsurface, that ends up moving offshore in filaments that can reach 200 km. Considering the

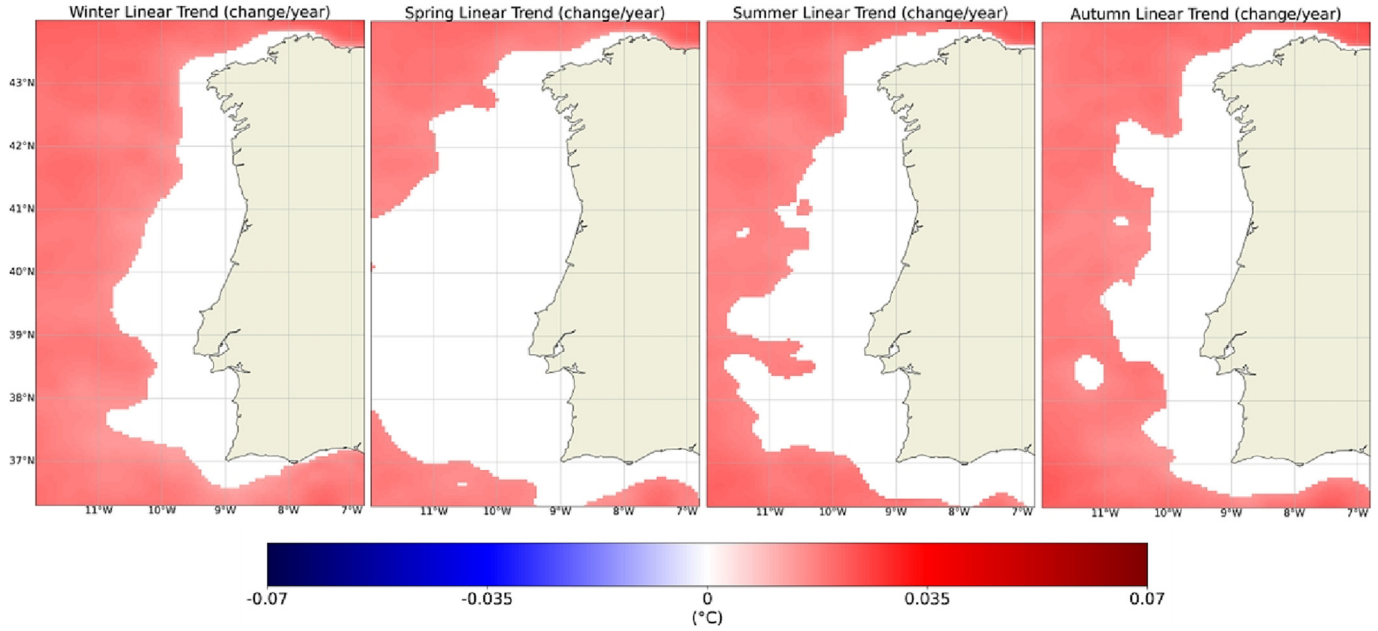

Fig. 11. Seasonal sea surface temperature trends from CCI, after a seasonality removal (based on annual seasonal averages). Only significant trends (95 % confidence interval) are presented.

whole period, a clear buffer effect was observed in the first 10 km to 20 km of coastal ocean and appeared to cause an attenuation of the *SST* increase in some regions up to 200 km offshore (Fig. 3). However, the extension of this buffer zone has changed over the years. By considering the decadal trends (Fig. 5), it is possible to have a better notion of the variation in the spatial extension of the buffer effect though time. During the 1990s, the existence of a buffer effect was not evident. In opposition, from the 2000s onwards, this effect started to get more intense, matching the coincident increasing trends in upwelling. Between 2000 and 2010, the area of buffer covered the coast from Setúbal region northwards and showed a seaward extension of about 30 km. For this same period, along the northwest region of Galicia, the buffer effect was observed up to 120 km offshore. In the decade from 2010 to 2019, this effect became much more intense and spatially generalized, showing an extension of >350 km offshore, that got reduced along the north and south margins of mainland. In addition to having decadal variations, this buffer for *SST* increase is present throughout the year along the coast and its extension varies seasonally, as shown in Fig. 11. Fig. 11 shows the *SST* trends as change/year (unlike the remaining figures), to allow a clearer observation of the spatial coverage of this phenomenon. Winter and Autumn seemed to be the seasons with the smallest seaward spatial extent of the buffer effect (maximum length of ≈225 km). The spatial extent of the effect along the southern coast of Portugal was particularly uniform during summer (≈75 km offshore), while in winter the effect was almost negligible along its easternmost region. The buffer effect achieved a greater offshore extension during spring, extending over 320 km, once again corroborating the possible influence of upwelling on this phenomenon. As Varela et al. (2018) concluded in a global analysis, upwelling has the potential to buffer ecosystems from climate change, depressing heating rates regardless of the region being considered. They showed that 92 % of the coastal upwelling areas presented lower warming than the adjacent coastal ocean. Therefore, it is likely that the lower increase in *SST* observed in this study is due to the buffering from upwelling that has been seen in other regions (Varela et al., 2018). The same authors also stated that for the Iberian Coast, differences between coast and ocean of −0.2 °C per decade were obtained. These values are close to those obtained in the present analysis. However, the dynamics of the underlying mechanism behind this buffering effect remained unknown (Varela et al., 2018) and, by integrating the analysis of atmospheric variables and ocean-atmosphere interactions, the present work allows to deepen the knowledge on this topic and to identify potential drivers of the observed patterns.

The present analysis has utilized high resolution long-term time series of *SST*, identifying the main temperature changes that have been occurring since 1982 along the Western Iberian Coast. The study constitutes a relevant scientific evidence base for the development of regional adaptation plans and to the implementation of local management and mitigation measures. This can be concretely translated, for example, into the management of fish stocks, such as sardines, an emblematic species of this region. *SST* increase could lead to a decrease in the sardine stock in the long term, which, would consequently have a negative socioeconomic impact on the Portuguese population (Ferreira et al., 2023). Understanding how these temperature variations have been influencing Iberian ecosystems will be essential to ensure the marine ecosystem's prosperity and food web structure.

5. Conclusions

This study quantified the main *SST* changes that have occurred along the Western Iberian Coast during the past four decades, using long-term *in situ* observations and satellite-derived time series. The first objective was to determine variations in the seasonality of *SST*. Results show that there has been an increase in the annual *SST* maximum for most of the offshore oceanic region. A delay in the timing of occurrence of the annual *SST* minimum value was found, primarily off the Galician coast. There was an increase in the number of days in which the *SST* was above average between 1982 and 2021, and in certain areas, the first day in these conditions has been anticipated. No significant changes in the seasonality of *SST* were observed near the coast.

The second objective was to quantify long-term *SST* trends and assess if these varied spatially along the coast. *SST* has been increasing along the Western Iberian coastal ocean, showing regional variations between 0.010 and 0.025 °C per year, for the period 1984–2019. Near the shore, significant decreasing trends were observed. The overall *SST* increase has been decelerating in recent decades in this region. This could be justified by an intensification of upwelling events and the simultaneous influence of several teleconnections, chiefly the *NAO* and the *WeMOI*.

The third objective was to examine the main drivers of the observed *SST* changes. Increasing air temperatures have been driving *SST* trends along the whole region of the Iberian Peninsula. The lack of significant changes near the coast of Western Iberian, regarding the seasonality and long-term trends, suggest that this region works as a buffer for *SST* changes because of the frequent occurrence of upwelling episodes.

This study is a valuable asset to the scientific evidence base supporting regional adaptation plans and the implementation of climate change mitigation measures, which ultimately will contribute to the well-being and resilience of Iberian populations and the proper functioning of their commercial and leisure activities.

Supplementary data to this article can be found online at https://doi.org/10.1016/j.scitotenv.2023.164193.

CRediT authorship contribution statement

Beatriz Biguino: Conceptualization, Data curation, Formal analysis, Investigation, Methodology, Writing – original draft. **Carlos Antunes:** Data curation, Formal analysis, Writing – review & editing. **Luísa Lamas:** Data curation, Formal analysis, Writing – review & editing. **Luke J. Jenkins:** Formal analysis, Writing – review & editing. **João Miguel Dias:** Formal analysis, Supervision, Writing – review & editing. **Ivan D. Haigh:** Formal analysis, Supervision, Writing – review & editing. **Ana C. Brito:** Conceptualization, Formal analysis, Supervision, Writing – review & editing, Project administration.

Data availability

Data will be made available on request.

Declaration of competing interest

The authors declare that they have no known competing financial interests or personal relationships that could have appeared to influence the work reported in this paper.

Acknowledgements

This study was supported by Fundação para a Ciência e Tecnologia (FCT) through the strategic project UIDB/04292/2020 awarded to MARE and through project LA/P/0069/2020 granted to the Associate Laboratory ARNET. The authors also acknowledge financial support to CESAM by FCT/MCTES (UIDP/50017/2020 + UIDB/50017/2020 + LA/P/0094/2020), through national funds. B. Biguino was supported by the doctoral Grant PRT/BD/152829/2021 funded by the FCT under the MIT Portugal Program. L.J. Jenkins was funded through the INSPIRE Doctoral Training Partnership by the Natural Environment Research Council (NERC) (NE/S007210/1) and co-sponsored by the JBA Trust. A.C. Brito was partially funded by FCT, through the Scientific Employment Stimulus Programme (CEECIND/0095/2017).

The *SST* satellite-derived data were extracted from the Copernicus Climate Change Service (https://cds.climate.copernicus.eu/cdsapp#!/dataset/satellite-sea-surface-temperature?tab=overview), NASA JPL PODAAC (https://podaac. jpl.nasa.gov/dataset/MUR-JPL-L4-GLOB-v4.1) and Copernicus ECMWF Climate Data Store (https://cds.climate.copernicus.eu/cdsapp#!/dataset/reanalysis-era5-single-levels?tab=overview), from where also the atmospheric data also retrieved.

References

Caputi, N., de Lestang, S., Feng, M., Pearce, A., 2009. Seasonal variation in the long-term warming trend in water temperature off the Western Australian coast. Mar. Freshw. Res. 60 (2), 129–139. https://doi.org/10.1071/MF08199.

Casey, K.S., Cornillon, P., 2001. Global and Regional Sea surface temperature trends. J. Clim. 3801–3818.

Chaidez, V., Dreano, D., Agusti, S., Duarte, C.M., Hoteit, I., 2017. Decadal trends in Red Sea maximum surface temperature. Sci. Rep. 7, 8144. https://doi.org/10.1038/s41598-017-08146-z.

Cheng, L., Abraham, J., Trenberth, K.E., Fasullo, J., Boyer, T., Locarnini, R., Zhang, B., Yu, F., Wan, L., Chen, X., Song, X., Liu, Y., Mann, M.E., Reseghetti, F., Simoncelli, S., Gouretski, V., Chen, G., Mishonov, A., Reagan, J., Zhu, J., 2021. Upper Ocean temperatures hit record high in 2020. Adv. Atmos. Sci. 38 (4), 523–530. https://doi.org/10.1007/s00376-021-0447-x.

Chin, T.M., Vazquez-Cuervo, J., Armstrong, E.M., 2017. A multi-scale high-resolution analysis of global sea surface temperature. Remote Sens. Environ. 200.

Commonwealth of Australia, 2022. Southern Oscillation Index (SOI) since 1876. http://www.bom.gov.au/climate/enso/soi/.

Copernicus, E.U., 2022. Iberia Biscay Ireland Sea Surface Temperature Trend Map from Observations Reprocessing. Https://Marine.Copernicus.Eu/Access-Data/Ocean-Monitoring-Indicators/Iberia-Biscay-Ireland-Sea-Surface-Temperature-Trend-Map.

Criado-Aldeanueva, F., Garcia-Lafuente, J., Navarro, G., Ruiz, J., 2009. Seasonal and interannual variability of the surface circulation in the eastern gulf of Cadiz (SW Iberia). Journal of Geophysical Research: Oceans 114 (1). https://doi.org/10.1029/2008JC005069.

Dalelane, C., Wetterdienst, D., 2019. Prediction of the North Atlantic oscillation index for the winter months December-January-February via nonlinear methods. Atmospheric and Oceanic Science Letters 12 (5), 320–328. https://doi.org/10.5194/egusphere-egu22-12628.

EPA, 2022. Climate Change Indicators: Sea Surface Temperature. https://www.epa.gov/climate-indicators/climate-change-indicators-sea-surface-temperature.

Ferreira, A., Dias, J., Brotas, V., Brito, A.C., 2022. A perfect storm: an anomalous offshore phytoplankton bloom event in the NE Atlantic (march 2009). Sci. Total Environ. 806. https://doi.org/10.1016/j.scitotenv.2021.151253.

Ferreira, A., Garrido, S., Costa, J.L., Teles-Machado, A., Brotas, V., Brito, A.C., 2023. What drives the recruitment of European sardine in Atlanto-Iberian waters (SW Europe)? Insights from a 22-year analysis Submitted.

Fortunato, B., Pinto, Lıgia, Oliveira, A., Ferreira, ao S., 2002. Tidally generated shelf waves off the western Iberian coast. Cont. Shelf Res. 22, 1935–1950.

García-Lafuente, J., Delgado, J., Criado-Aldeanueva, F., Bruno, M., del Río, J., Miguel Vargas, J., 2006. Water mass circulation on the continental shelf of the Gulf of Cádiz. Deep-Sea Research Part II: Topical Studies in Oceanography 53 (11 − 13), 1182–1197. https://doi.org/10.1016/j.dsr2.2006.04.011.

García-Monteiro, S., Sobrino, J.A., Julien, Y., Sòria, G., Skokovic, D., 2022. Surface temperature trends in the Mediterranean Sea from MODIS data during years 2003–2019. Reg. Stud. Mar. Sci. 49. https://doi.org/10.1016/j.rsma.2021.102086.

Garcia-Soto, C., Cheng, L., Caesar, L., Schmidtko, S., Jewett, E.B., Cheripka, A., Rigor, I., Caballero, A., Chiba, S., Báez, J.C., Zielinski, T., Abraham, J.P., 2021. An Overview of Ocean Climate Change Indicators: Sea Surface Temperature, Ocean Heat Content, Ocean pH, Dissolved Oxygen Concentration, Arctic Sea Ice Extent, Thickness and Volume, Sea Level and Strength of the AMOC (Atlantic Meridional Overturning Circulation). Frontiers in Marine Science. vol. 8. Frontiers Media S.A.. https://doi.org/10.3389/fmars.2021.642372.

Getahun, Y.S., Li, M.H., Pun, I.F., 2021. Trend and change-point detection analyses of rainfall and temperature over the Awash River basin of Ethiopia. Heliyon 7 (9), e08024. https://doi.org/10.1016/j.heliyon.2021.e08024.

Good, S.A., Embury, O., Bulgin, C.E., Mittaz, J., 2019. ESA Sea Surface Temperature Climate Change Initiative (SST_cci): Level 4 Analysis Climate Data Record, Version 2.0. Centre for Environmental Data Analysis.

Hartmann, D.L., Klein Tank, A.M.G., Rusticucci, M., Alexander, L.V., Brönnimann, S., Charabi, Y., Dentener, F.J., Dlugokencky, E.J., Easterling, D.R., Kaplan, A., Soden, B.J., Thorne, P.W., Wild, M., Zhai, P.M., 2013. Observations: Atmosphere and Surface. In: Stocker, T.F., Qin, D., Plattner, G.-K., Tignor, M., Allen, S.K., Boschung, J., Nauels, A., Xia, Y., Bex, V., Midgley, P.M. (Eds.), Climate Change 2013: The Physical Science Basis. Contribution of Working Group I to the Fifth Assessment Report of the Intergovernmental Panel on Climate Change. Cambridge University Press, Cambridge, United Kingdom and New York, NY, USA.

Hastings, R.A., Rutterford, L.A., Freer, J.J., Collins, R.A., Simpson, S.D., Genner, M.J., 2020. Climate Change Drives Poleward Increases and Equatorward Declines in Marine Species. Curr. Biol. 30 (8), 1572–1577. https://doi.org/10.1016/j.cub.2020.02.043 e2.

Hereher, Mohamed E., 2022. Climate change during the third millennium—the Gulf cooperation council countries. Sustainability 14 (21), 14181. https://doi.org/10.3390/su142114181.

Hersbach, H., Bell, B., Berrisford, P., Biavati, G., Horányi, A., Muñoz Sabater, J., Nicolas, J., Peubey, C., Radu, R., Rozum, I., Schepers, D., Simmons, A., Soci, C., Dee, D., Thépaut, J.-N., 2018. ERA5 hourly data on single levels from 1959 to present. Copernicus Climate Change Service (C3S) Climate Data Store (CDS).

Hu, S., Xie, S.P., Liu, W., 2020. Global pattern formation of net ocean surface heat flux response to greenhouse warming. J. Clim. 33 (17), 7503–7522. https://doi.org/10.1175/JCLI-D-19-0642.1.

IPCC, 2019. IPCC Special Report on the Ocean and Cryosphere in a Changing Climate. In: Pörtner, H.O., Roberts, D.C., Masson-Delmotte, V., Zhai, P., Tignor, M., Poloczanska, E., Mintenbeck, K., Alegría, A., Nicolai, M., Okem, A., Petzold, J., Rama, B., Weyer, N.M. (Eds.), Intergovernmental Panel on Climate Change . https://www.ipcc.ch/srocc/chapter/summary-for-policymakers/.

IPCC, 2021. Summary for Policymakers. In: Masson-Delmotte, V., Zhai, P., Pirani, A., Connors, S.L., Péan, C., Berger, S., Caud, N., Chen, Y., Goldfarb, L., Gomis, M.I., Huang, M., Leitzell, K., Lonnoy, E., Matthews, J.B.R., Maycock, T.K., Waterfield, T., Yelekçi, O., Yu, R., Zhou, B. (Eds.), Climate Change 2021: The Physical Science Basis. Contribution of Working Group I to the Sixth Assessment Report of the Intergovernmental Panel on Climate Change. Cambridge University Press, pp. 3–32 https://doi.org/10.1017/9781009157896.001.

Jiang, F., Zhang, W., 2022. Understanding the complicated relationship between ENSO and wintertime north tropical Atlantic SST variability. Geophys. Res. Lett. 49 (5). https://doi.org/10.1029/2022GL097889.

Jing, Y., Li, Y., Xu, Y., Fan, G., 2019. Influences of different definitions of the winter NAO index on NAO action centers and its relationship with SST. Atmospheric and Oceanic Science Letters 12 (5), 320–328. https://doi.org/10.1080/16742834.2019.1628607.

Jo, A.R., Lee, J.Y., Timmermann, A., Jin, F.F., Yamaguchi, R., Gallego, A., 2022. Future amplification of sea surface temperature seasonality due to Enhanced Ocean stratification. Geophys. Res. Lett. 49 (9). https://doi.org/10.1029/2022GL098607.

JPL MUR MEaSUREs Project, 2015. GHRSST Level 4 MUR Global Foundation Sea Surface Temperature Analysis. Ver. 4.1. PO.DAAC, CA, USA.

Kessler, A., Goris, N., Lauvset, S.K., 2022. Observation-Based Sea surface temperature trends in Atlantic large marine ecosystems. Prog. Oceanogr. 208. https://doi.org/10.1016/j.pocean.2022.102902.

Knight, J.R., Folland, C.K., Scaife, A.A., 2006. Climate impacts of the Atlantic multidecadal oscillation. Geophys. Res. Lett. 33 (17). https://doi.org/10.1029/2006GL026242.
Krichak, S.O., Alpert, P., 2005. Decadal trends in the East Atlantic-West Russia pattern and Mediterranean precipitation. Int. J. Climatol. 25 (2), 183–192. https://doi.org/10.1002/joc.1124.
Lana, X., Burgueño, A., Martínez, M.D., Serra, C., 2016. Complexity and predictability of the monthly western mediterranean oscillation index. Int. J. Climatol. 36 (6), 2435–2450. https://doi.org/10.1002/joc.4503.
Li, J., Tan, S., Wei, Z., Chen, F., Feng, P., 2014. A new method of change point detection using variable fuzzy sets under environmental change. Water Resour. Manag. 28 (14), 5125–5138. https://doi.org/10.1007/s11269-014-0798-5.
Lima, F.P., Wethey, D.S., 2012. Three decades of high-resolution coastal sea surface temperatures reveal more than warming. Nat. Commun. 3. https://doi.org/10.1038/ncomms1713.
Liu, X., Yao, F., 2022. Relationship of the warming of Red Sea surface water over 140 years with external heat elements. Journal of Marine Science and Engineering 10 (7). https://doi.org/10.3390/jmse10070846.
Mantas, V.M., Pereira, A.J.S.C., Marques, J.C., 2019. Partitioning the ocean using dense time series of earth observation data. Regions and natural boundaries in the Western Iberian Peninsula. Ecol. Indic. 103 (November 2018), 9–21. https://doi.org/10.1016/j.ecolind.2019.03.045.
Merchant, C.J., Embury, O., Bulgin, C.E., Block, T., Corlett, G.K., Fiedler, E., Good, S.A., Mittaz, J., Rayner, N.A., Berry, D., Eastwood, S., Taylor, M., Tsushima, Y., Waterfall, A., Wilson, R., Donlon, C., 2019. Satellite-based time-series of sea-surface temperature since 1981 for climate applications. Scientific Data 6 (223).
Meshram, S.G., Singh, V.P., Meshram, C., 2017. Long-term trend and variability of precipitation in Chhattisgarh State, India. Theoretical and Applied Climatology 129 (3–4), 729–744. https://doi.org/10.1007/s00704-016-1804-z.
Minnett, P.J., Alvera-Azcárate, A., Chin, T.M., Corlett, G.K., Gentemann, C.L., Karagali, I., Li, X., Marsouin, A., Marullo, S., Maturi, E., Santoleri, R., Saux Picart, S., Steele, M., Vazquez-Cuervo, J., 2019. Half a century of satellite remote sensing of sea-surface temperature. Remote Sens. Environ. 233. https://doi.org/10.1016/j.rse.2019.111366.
NOAA, 2012. East Atlantic (EA). National Weather Service, Climate Prediction Center. https://www.cpc.ncep.noaa.gov/data/teledoc/ea.shtml.
NOAA/ESRL, 2022. Atlantic Multidecadal Oscillation (AMO). Https://Stateoftheocean.Osmc.Noaa.Gov/Atm/Amo.Php.
Pastor, F., Valiente, J.A., Khodayar, S., 2020. A warming Mediterranean: 38 years of increasing sea surface temperature. Remote Sens. 12 (17). https://doi.org/10.3390/RS12172687.
Peliz, Á., Dubert, J., Santos, A.M.P., Oliveira, P.B., Le Cann, B., 2005. Winter upper ocean circulation in the Western Iberian Basin - fronts, eddies and poleward flows: an overview. Deep-Sea Research Part I: Oceanographic Research Papers 52 (4), 621–646. https://doi.org/10.1016/j.dsr.2004.11.005.
Prigent, A., Imbol Koungue, R.A., Lübbecke, J.F., Brandt, P., Latif, M., 2020. Origin of weakened Interannual Sea surface temperature variability in the southeastern tropical Atlantic Ocean. Geophys. Res. Lett. 47 (20). https://doi.org/10.1029/2020GL089348.
Relvas, P., Barton, E.D., Dubert, J., Oliveira, P.B., Peliz, Á., da Silva, J.C.B., Santos, A.M.P., 2007. Physical oceanography of the western Iberia ecosystem: latest views and challenges. Prog. Oceanogr. 74 (2–3), 149–173. https://doi.org/10.1016/j.pocean.2007.04.021.
Ruela, R., Sousa, M.C., deCastro, M., Dias, J.M., 2020. Global and regional evolution of sea surface temperature under climate change. Glob. Planet. Chang. 190, 103190. https://doi.org/10.1016/j.gloplacha.2020.103190.
Sakalli, A., Başusta, N., 2018. Sea surface temperature change in the Black Sea under climate change: a simulation of the sea surface temperature up to 2100. Int. J. Climatol. 38 (13), 4687–4698. https://doi.org/10.1002/joc.5688.
Santos, F., Gomez Gesteira, M., deCastro, M., 2011. Coastal and oceanic SST variability along the western Iberian Peninsula. Cont. Shelf Res. 31 (19–20), 2012–2017. https://doi.org/10.1016/j.csr.2011.10.005.
Santos, F., Gómez-Gesteira, M., deCastro, M., Álvarez, I., 2012. Variability of coastal and ocean water temperature in the upper 700 m along the Western Iberian Peninsula from 1975 to 2006. PLoS One 7 (12). https://doi.org/10.1371/journal.pone.0050666.
Santos, L.C., Lima, M.M., Bento, V.A., Nunes, S.A., DaCamara, C.C., Russo, A., Soares, P.M.M., Trigo, R.M., 2023. An evaluation of the atmospheric instability effect on wildfire danger using ERA5 over the Iberian Peninsula. Fire 6 (3), 120. https://doi.org/10.3390/fire6030120.
Sent, G., Biguino, B., Favareto, L., Cruz, J., Sá, C., Dogliotti, A.I., Brotas, V., Brito, A.C., 2021. Deriving Water Quality Parameters Using Sentinel-2 Imagery: A Case Study in the Sado Estuary. Remote Sensing, Portugal.
Serinaldi, F., Kilsby, C.G., 2016. The importance of prewhitening in change point analysis under persistence. Stoch. Env. Res. Risk A. 30 (2), 763–777. https://doi.org/10.1007/s00477-015-1041-5.
Singh, R., Sah, S., Das, B., Potekar, S., Chaudhary, A., Pathak, H., 2021. Innovative trend analysis of spatio-temporal variations of rainfall in India during 1901–2019. Theor. Appl. Climatol. 145 (1–2), 821–838. https://doi.org/10.1007/s00704-021-03657-2.
Sousa, M.C., deCastro, M., Alvarez, I., Gomez-Gesteira, M., Dias, J.M., 2017. Why coastal upwelling is expected to increase along the western Iberian Peninsula over the next century? Sci. Total Environ. 592, 243–251. https://doi.org/10.1016/j.scitotenv.2017.03.046.
Teles-Machado, A., Peliz, A., McWilliams, J.C., Cardoso, R.M., Soares, P.M.M., Miranda, P.M.A., 2015. On the year-to-year changes of the Iberian poleward current. Journal of Geophysical Research: Oceans 120, 4980–4999. https://doi.org/10.1038/175238c0.
Utrabo-Carazo, E., Azorin-Molina, C., Serrano, E., Aguilar, E., Brunet, M., Guijarro, J.A., 2022. Wind stilling ceased in the Iberian Peninsula since the 2000s. Atmos. Res. 272. https://doi.org/10.1016/j.atmosres.2022.106153.
Varela, R., Lima, F.P., Seabra, R., Meneghesso, C., Gómez-Gesteira, M., 2018. Coastal warming and wind-driven upwelling: a global analysis. Sci. Total Environ. 639, 1501–1511. https://doi.org/10.1016/j.scitotenv.2018.05.273.
Visbeck, M.H., Hurrell, J.W., Polvani, L., Cullen, H.M., 2001. The North Atlantic Oscillation: Past, present, and future. In PNAS November 6 (23).. www.pnas.orgcgidoi10.1073pnas.231391598.
Wu, Z., Jiang, C., Conde, M., Chen, J., Deng, B., 2020. The long-term spatiotemporal variability of sea surface temperature in the Northwest Pacific and China offshore. Ocean Sci. 16 (1), 83–97. https://doi.org/10.5194/os-16-83-2020.
Xu, Z., Ji, F., Liu, B., Feng, T., Gao, Y., He, Y., Chang, F., 2021. Long-term evolution of global sea surface temperature trend. Int. J. Climatol. 41 (9), 4494–4508. https://doi.org/10.1002/joc.7082.
Zeng, Z., Ziegler, A.D., Searchinger, T., Yang, L., Chen, A., Ju, K., Piao, S., Li, L.Z.X., Ciais, P., Chen, D., Liu, J., Azorin-Molina, C., Chappell, A., Medvigy, D., Wood, E.F., 2019. A reversal in global terrestrial stilling and its implications for wind energy production. Nat. Clim. Chang. 9 (12), 979–985. https://doi.org/10.1038/s41558-019-0622-6.